ANALYTICAL SCIENCES JULY 2003, VOL. 19

Notes

Single Particle Confocal Fluorescence Spectroscopy in Microchannels: Dependence of Burst Width and Burst Area Distributions on Particle Size and Flow Rate

Joshua B. EDEL and Andrew J. de MELLO†

Department of Chemistry, Imperial College London, South Kensington, London, SW7 2AZ, U.K.

This article presents a non-invasive, optical technique for measuring particulate flow within microfluidic channels. Confocal fluorescence detection is used to probe single fluorescently labeled microspheres (200 – 930 nm diameter) passing through a focused laser beam at a variety of flow rates (100 – 1000 nL/min). Simple statistical methods are subsequently used to investigate the resulting fluorescence bursts and generate single-particle burst width and burst area distributions. Analysis of such distributions demonstrates that the average burst width and burst area decrease as particle size increases. In addition, both burst width and burst area (for a given particle size) are observed to decrease as volumetric flow rate is increased. The dependence of such distributions on particle size is proposed as a potential route to sizing single particles and molecules in microfluidic systems.

(Received February 21, 2003; Accepted April 14, 2003)

The first successful detection of individual molecules in solution was presented by Hirschfield in 1976.[1] In these experiments, single γ-globulin antibodies (labeled with approximately 100 fluorescein isothiocyanate molecules) were detected, by emission of a burst of photons, as they diffused through an excitation volume defined by a laser beam. Since this time, significant advances in ultra-sensitive detection of fluorescent molecules in liquids have been made allowing the detection of a wide variety of species at extremely low analytical concentrations. At present, there are a number of distinct approaches applied to the detection of single fluorophores in solution.[2-5] A popular method to achieve single-molecule detection sensitivity adopts the principle of confocal detection.[6-9] In this, a femtolite probe volume is defined by a focused laser beam (near the diffraction limit) and a confocal pinhole. As a molecule diffuses through this volume it emits a burst of fluorescence photons, which can be collected and detected. Importantly, the use of femtolite probe volumes minimizes background signals, which originate from Rayleigh and Raman scattering by solvent molecules, due to the reduced number of such molecules in small volumes. A different approach to efficient single molecule detection in solution involves enlarging the focal region of the laser beam to create a detection volume in the low picoliter range. Hydrodynamic focusing of a narrow stream within a sheath flow (orthogonal to excitation) then ensures that the entire sample is delivered to the probe region.[10] Under appropriate conditions, each molecule within the sample can be detected sequentially and with high efficiency. This approach is conventionally termed single-molecule flow cytometry (SMFC). In SMFC, individual molecules are motivated within the sample stream at the same rate, and experience the same radiation field during their passage through the detection volume. This allows the identification of molecular size on the basis of fluorescence burst characteristics. For example, DNA fragment sizing, DNA sequencing and hybridization analysis based on single molecule detection have been demonstrated, and hold great promise for improving sensitivity and reducing analysis times in such assays.[2]

A primary disadvantage with SMFC methods is the large background signal that arises when the probe volume is enlarged to the picoliter scale. This can often be larger than the fluorescence signal from the target molecule, and is directly related to the increase in the number of solvent/impurity molecules in the probe volume. Consequently, a number of methods to suppress background signals have been proposed. These include, pulsed laser excitation coupled with time-gated detection[2] (to discriminate between fluorescence and scattering signals) and photobleaching of the sheath flow upstream of the detection volume (to remove the luminescence background from impurity species).[11,12] Although successful, these methods add a certain degree of experimental complexity. Consequently, in this communication we propose a simpler method that can potentially be used to size single particles or molecules in free solution. The approach utilizes standard confocal fluorescence microscopy (incorporating femtoliter detection volumes) to detect single molecules. Although, the detection efficiency (in terms of the fraction of all molecules detected) is inferior to that achieved in SMFC methods, the approach can be used to size particles flowing through femtoliter detection volumes, without the need to use hydrodynamic focusing and a sheath flow, or complex background suppression techniques. To assess feasibility of this concept we present initial studies relating to the detection of nanometer sized particles flowing though microchannels structured in planar glass chips.

Experimental

Precise details of the experimental system are described elsewhere.[9] Briefly, the excitation source used in all experiments is a 488 nm CW air-cooled argon ion laser (Omnichrome; Melles Griot, Cambridge, UK). Glass neutral density filters (0.2 – 4 o.d.) were used to attenuate the laser

† To whom correspondence should be addressed.
E-mail: a.demello@ic.ac.uk

intensity as required (Newport Ltd., Newbury, UK). A dichroic mirror (505DRLP02; Omega Optical, Brattleboro, VT, USA) is oriented at 45˚ to reflect 488 nm radiation and so define a vertical axis, normal to the surface of the optical table. An infinity corrected, high numerical aperture (NA) microscope objective (Fluar 100×/1.3 NA, oil immersion; Carl Zeiss Ltd., Welwyn Garden City, UK) brings the light to a tight focus within the sample chamber. The collimated laser beam has a $1/e^2$ diameter of 2.5 mm. The focused laser spot defines an approximate probe volume of 0.42 fL.

Microfluidic devices were manufactured in-house and comprised a thermally bonded structured glass substrate containing the microchannel network. Microfluidic channel patterns were transferred onto a glass wafer pre-coated with positive photoresist and chromium (Nanofilm, Westlake Village, CA, USA) using a direct-write photolithographic system (DWL2.0, Heidelberg Instruments, Heidelberg, Germany). Typical channel widths ranged from 5 – 50 μm. The exposed photoresist was then removed using a 5:1 ratio of developing agent (Microposit, Coventry, UK) to water. This was followed by a chromium etching procedure using a Lodyne etch (Microchem Systems, Coventry, UK). The etched substrates were finally rinsed in 18 MΩ water and H_2SO_4–H_2O_2 (50:50). Coverplates were bonded to etched substrates by heating in a high temperature oven to a maximum of 610˚C. The top plate was then optically polished down to a thickness of ~150 μm. Optical polishing of the coverplate was performed to reduce the substrate thickness below the working distance of the microscope objective (~150 μm). Fluidic access holes were then etched into the fluidic network *via* deep reactive ion etching using an 8 M solution of sodium hydroxide and an applied voltage of 120 V.

The completed microchip was placed on a translation stage and appropriately aligned under the microscope objective. Under a hydrodynamic pumping regime the analyte velocity is highly dependent on position perpendicular to the flow direction. Consequently, in all experiments, the confocal probe volume was positioned at the center of the microchannel to minimize variations in analyte velocity through the probe volume. A syringe pump (Harvard Apparatus, Cambridge, MA, USA) is used to deliver solutions at various flow rates from either a 500-μL or 50-μL gastight syringe into the capillary tubing. Typical flow rates used for the current experiments ranged from 0.05 – 20 μL/min. Fluorescence emitted by the sample is collected by the same high NA objective and transmitted through the dichroic mirror. An emission filter (515EFLP; Omega Optical, UK) removes any residual excitation light. A plano-convex lens (+50.2F; Newport Ltd.) focuses the fluorescence onto a precision pinhole (25 μm; Melles Griot) placed immediately in front of the detector. The pinhole is positioned in the confocal plane of the microscope objective. The detector is a silicon avalanche photodiode operating in single-photon counting mode (SPCM-AQR-131; EG & G Canada, Vaudreuil, Quebec, Canada). The dark count rate on average was well below 60 Hz. The precision pinhole and detector are mounted on an XYZ translation stage to allow for fine adjustment of the incoming radiation. The electronic signal from the detector is coupled to a multi channel scaler (MCS-PCI; EG & G), running on a Pentium PC.

A program written in Matlab 6.5 (Mathworks, Cambridge, UK) was used to determine peak heights, areas, widths, and location. Briefly, the program searches for a given peak maximum above a specific threshold value which can be defined as three standard deviations from the mean count rate, *i.e.* $n_{threshold} = \mu + 3\sqrt{\mu}$. Adoption of a threshold that lies 3 standard deviations above the mean yields confidence limits greater than 99%. Once a peak is located, the peak area is determined by analyzing a specified number of bins either side of the peak maximum until the background threshold value is reached. The program then searches for the next peak and continuously repeats until all peaks are accounted for. The mean and standard deviation are then calculated for burst heights, areas, and widths. The distribution plots are histograms generated from all sampled bursts of a given size and flow velocity.

Fluorescent microbeads (yellow/green Fluospheres®, Molecular Probes; Europe B.V.) having a mean diameter of 930 nm, 500 nm, and 200 nm, respectively were used for all experiments. Absorption and emission maxima were 505 nm and 515 nm, respectively. Stock solutions were diluted by a factor of 2000. All dilutions were performed in TBE (tris–borate–EDTA) buffer. The TBE buffer was prepared at 0.1 × concentration (8.9 mM each of tris(methoxy)aminomethane and boric acid, 0.2 mM in ethylenediaminetretraacetic acid; prepared from a solid TBE mixture; Fluka Chemicals) in 18 MΩ deionized water. The beads were sonicated for 10 min immediately before use to ensure the beads did not coagulate. Typical working solutions had a concentration of 2.3×10^7 beads/cm^3 (effective concentration of 10 ng/L). This is equivalent to a 2000 fold dilution of the stock solution.

Results and Discussion

Fluorescent burst scans from 930 nm Fluospheres at volumetric flow rates of 50 nL/min – 1000 nL/min have been shown previously by Edel *et al*.[8] Figure 1 shows burst scans for 930 nm, 500 nm, and 200 nm Fluospheres at flow rates of 100, 1000, and 5000 nl/min, respectively. It is observed that individual bursts vary significantly in height. This is primarily caused by a range of possible particle trajectories through the probe volume. Figure 2a shows histograms of burst width distributions of 930 nm Fluosphere solutions traveling at volumetric flow rates ranging between 5 μL/min and 100 nL/min through a microfluidic channel. The microchannel was 10 μm wide at the bottom (40 μm wide at the top) and 15 μm deep. At high flow rates, a relatively even distribution of particle widths is observed (*e.g.* Fig. 2a(i)), whereas at a much lower flow rate (*e.g.* Fig. 2a(ii)) the particle width distribution becomes heavily skewed towards larger burst widths. These effects can be explained as follows: at lower flow rates, diffusion of the particles through the probe volume is the dominating factor in determining the trajectory through the probe volume hence the burst widths are be expected to be predominately random. The random behavior of the particle burst widths is clearly seen in Fig. 2a(iii). For all experiments the probe volume width (defined by the diffraction limited beam waist diameter) was measured to be approximately 1 μm, hence the laser beam was only a factor of 40 times smaller than the microfluidic channel. At higher flow rates diffusion is negligible with respect to bulk flow velocities and hence all particles travel through the probe volume with a predominantly constant trajectory; hence a more even distribution of burst widths is expected. This behavior is supported by both theory and analysis of the single-particle fluorescence burst scans. The diffusion coefficient of the 930 nm sphere is calculated to be 4.9×10^{-13} m^2/s. This yields a diffusion time (the characteristic molecular residence time in the probe volume for a static sample) of approximately 20 ms. Experimentally determined autocorrelation curves for 930-nm particles traveling at 5000

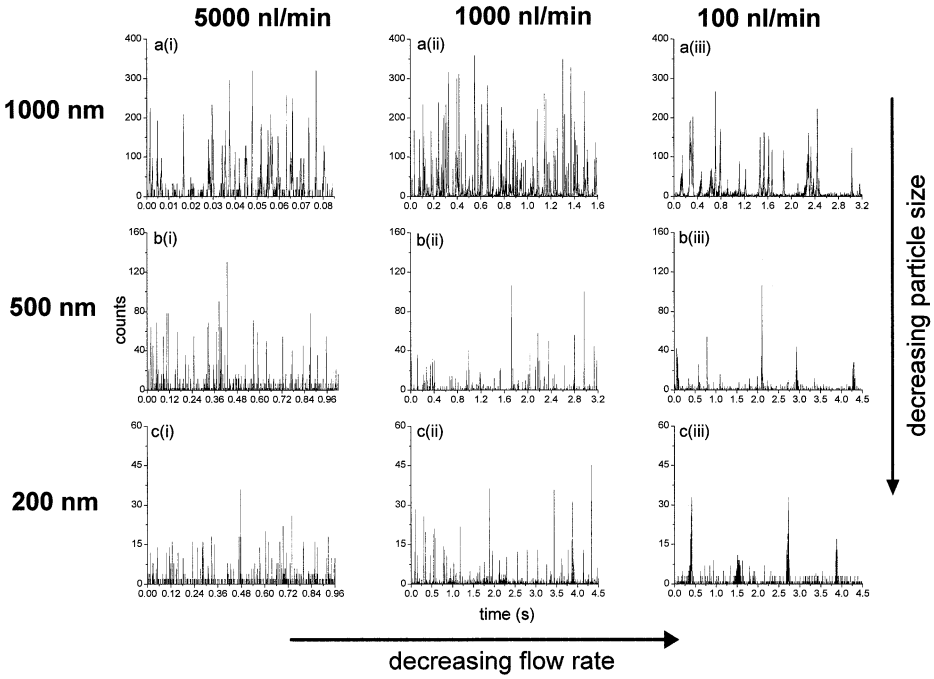

Fig. 1 Representative single-particle fluorescence burst scans for 930 nm, 500 nm, and 200 nm Fluospheres at flow rates of 100, 1000, and 5000 nl/min, respectively.

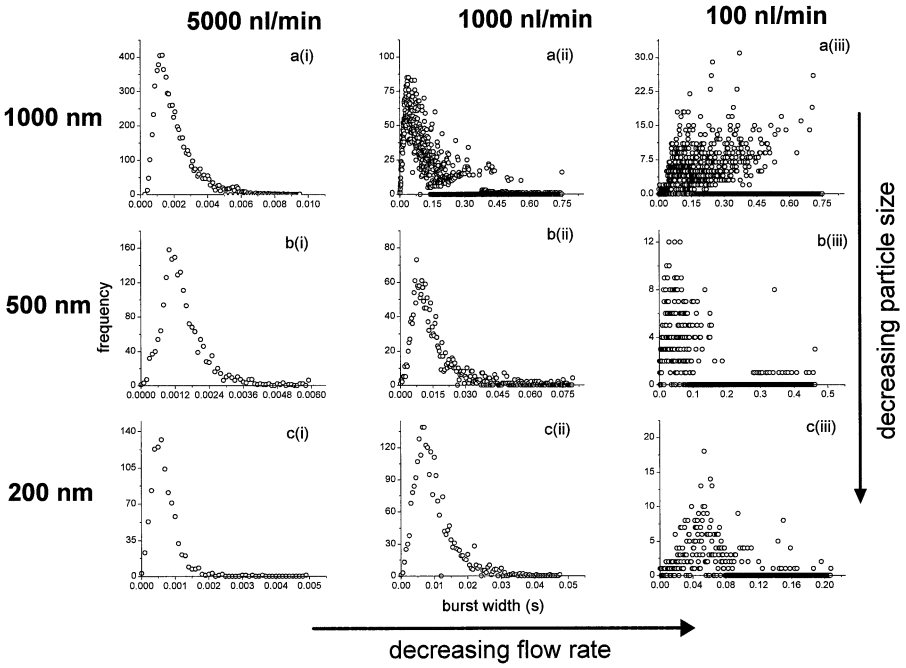

Fig. 2 Histograms of burst width distributions of 930 nm, 500 nm, and 200 nm Fluosphere solutions travelling at flow rates ranging between 5000 nL/min and 100 nL/min through a microfluidic channel.

nL/min through the probe volume yield a diffusion time of approximately 18 ms (in close agreement with the theoretical value). Both values are significantly higher than the beam transit time (200 μs), and thus demonstrate that diffusional effects are negligible in this system at higher flow rates.

Figures 2b and c show similar trends for 500 nm and 200 nm Fluospheres (with flow rates identical to those in Fig. 2a). As expected the overall burst heights are not only smaller, but the burst widths are also much smaller. It is interesting to note that the relative standard deviation is slightly larger when compared to the data obtained for 930 nm Fluospheres. This can be attributed to a greater domination of diffusive motion for smaller particles at a higher flow rate. Figures 3a – c show histograms of burst area distributions of Fluosphere solutions traveling at volumetric flow rates ranging between 5000 nL/min and 100 nL/min. The defined peak distribution observed at high flow rates disappears quickly as the flow rate is decreased. This is observed since histograms are binned into 1 count intervals;

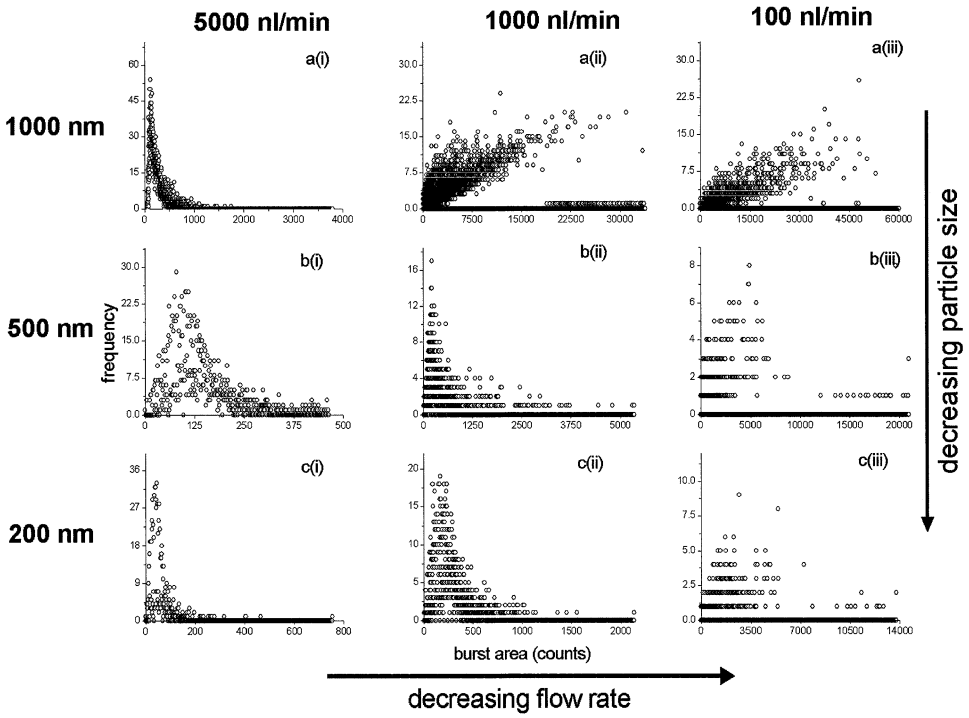

Fig. 3 Histograms of burst area distributions of 930 nm, 500 nm, and 200 nm Fluosphere solutions travelling at flow rates ranging between 5000 nL/min and 100 nL/min through a microfluidic channel.

Table 1 Average burst widths (ms) and average burst areas (counts) for 930 nm, 500 nm, and 200 nm Fluospheres at volumetric flow rates of 5000, 1000 and 100 nL/min

	Fluorescence burst width/ms			Fluorescence burst area/counts		
	5000	1000	100	5000	1000	100
930 nm Fluosphere	2.02	105	255	254	6000	16500
500 nm Fluosphere	1.60	16	72	181	506	2700
200 nm Fluosphere	0.88	5	60	79	317	2000

hence, the distribution or standard deviation is expected to be larger than when compared to the burst widths.

Table 1 summarizes the average burst width (ms) and average burst area (counts) for the 3 particle sizes given at 3 flow rates. It can be seen that the average burst width and burst area decrease as particle size increases. This effect is most noticeable at high volumetric flow rates (where diffusional effects are negligible) and most probably occurs due to the fact that for the same velocity a larger particle is associated with the probe volume for a longer time by virtue of its size. In addition, both burst width and burst area (for a given particle size) are observed to decrease as volumetric flow rate is increased.

The simplicity of the described approach for obtaining well defined burst width distributions could be extremely valuable for single particle sizing experiments. As stated, established fluorescence methods for single molecule sizing incorporate elaborate procedures for optimizing molecular collection efficiencies (*e.g.* through the use of sheath streams, microcapillaries, microdroplet streams and enlarged probe volumes). These approaches are not without consequences, as special techniques must be utilized to suppress the background count rates, which can be much larger than the signal from a single chromophore. In the approach taken herein, we are able to use a sub femtoliter probe volume while controlling the shape of the distribution without making any changes to a basic confocal microscopic experiment.

Figure 4 shows the peak height standard deviation at various flow rates for 930 nm, 500 nm, and 200 nm Fluospheres in a microfluidic channel. At a flow rate of 5000 nL/min a relative standard deviation of 35% was obtained for the 930 nm spheres. This was determined from an accumulation of over 200 bursts. As the particle size decreases there is a general trend for the RSD to increase. The relative standard error in this case was 2.1%. This value could be further decreased by increasing the number of bursts sampled. Decreasing the microfluidic channel width to 5 μm proved to decrease the relative standard deviation even further.[13] This effect will be described in more detail in a following publication. On average it took approximately 600 μs of recorded data to obtain 200 bursts at a flow rate of 5000 nL/min. Calculations at higher flow rates were not performed as acquisition dwell times below 25 μs are necessary to obtain sufficient data points per burst.

The approach used herein to characterize burst width and area distributions is facilitated by the fact that the amount (or number) of fluorescent molecules contained within a given particle is proportional to the particle size, and thus burst distribution characteristics at a given flow rate are directly related to particle size. This method would be generally useful in applications were species are distinguishable by the quantity of fluorophore labeled to them. For example, fluorescently labeled DNA strands have a distinguishable quantity of labeling sites which are characteristic of size. Hence, a given burst distribution can be directly correlated to a given strand length.

In conclusion, it is seen that analysis of single particle fluorescence burst scans allows an assessment of particle size

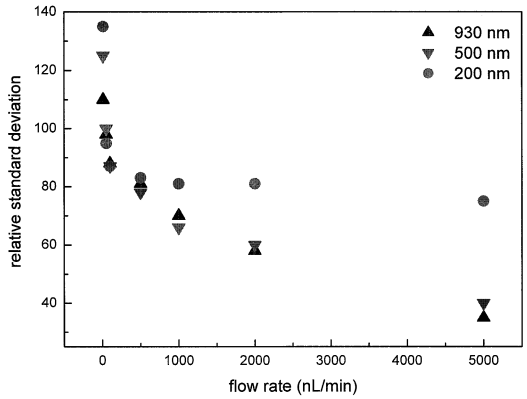

Fig. 4 Variation of peak height relative standard deviation as a function of volumetric flow rate.

and particle velocity in microchannels *via* fluorescence burst width and fluorescence burst area distibutions. Current studies are addressing a theoretical analysis of molecular distributions in microfluidic channels traveling through a sub femtoliter probe volume at a variety of volumetric flow rates.

Acknowledgements

J. B. E. acknowledges the receipt of an Overseas Research Studentship from the UK Government.

References

1. T. Hirschfeld, *Appl. Optics*, **1976**, *15*, 2965.
2. W. P. Ambrose, P. M. Goodwin, J. H. Jett, A. Van Orden, J. H. Werner, and R. A. Keller, *Chem. Rev*., **1999**, *99*, 2929.
3. W. P. Ambrose, R. L. Affleck, P. M. Goodwin, R. A. Keller, J. C. Martin, J. T. Petty, J. A. Schecker, and M. Wu, *Exp. Tech. Phys*., **1995**, *41*, 237.
4. B. B. Haab and R. A. Mathies, *Anal. Chem*., **1999**, *71*, 5137.
5. K. Kneipp, H. Kneipp, R. Manoharan, I. Itzkan, R. R. Dasari, and M. S. Feld, *Bioimaging*, **1998**, *6*, 104.
6. M. M. Ferris and K. L. Rowlen, *Rev. Sci. Instrum*., **2002**, *73*, 2404.
7. M. Maus, M. Cotlet, J. Hofkens, T. Gensch, F. C. De Schryver, J. Schaffer, and C. A. M. Seidel, *Anal. Chem*., **2001**, *73*, 2078.
8. J. B. Edel, E. K. Hill, and A. J. de Mello, *Analyst*, **2001**, *126*, 1953.
9. E. K. Hill and A. J. deMello, *Analyst*, **2000**, *125*, 1033.
10. D. C. Nguyen, R. A. Keller, J. H. Jett, and J. C. Martin, *Anal. Chem*., **1987**, *59*, 2158.
11. C. Eggeling, J. Widengren, R. Rigler, and C. A. M. Seidel, *Anal. Chem*., **1998**, *70*, 2651.
12. R. L. Affleck, W. P. Ambrose, J. N. Demas, P. M. Goodwin, J. A. Schecker, J. M. Wu, and R. A. Keller, *Anal. Chem*., **1996**, *68*, 2270.
13. J. B. Edel, unpublished results, **2003**.